Diagn Interv Radiol 2019; 25:204–209



CHEST IMAGING

ORIGINAL ARTICLE

# Fast kilovoltage-switching dual-energy CT offering lower x-ray dose than single-energy CT for the chest: a quantitative and qualitative comparison study of the two methods of acquisition

Osman Melih Topçuoğlu
Başar Sarıkaya

**PURPOSE**
We aimed to compare the size-specific dose estimates (SSDE), computed tomography (CT) dose indices and image quality parameters of the chest CTs obtained with fast kilovoltage-switching (FKS) dual-energy (DE) CT versus those with single-energy (SE) CT.

**METHODS**
Patients who had chest SECT within the last 6 months were prospectively scanned with chest FKS-DECT. Quantitative comparison was made by calculating the mean SSDE, $CTDI_{vol}$, contrast, noise, contrast-to-noise ratio (CNR), and signal-to-noise ratio (SNR) for both acquisitions. Two radiologists evaluated the chest SECT and DECT images qualitatively blinded to the technique used. The paired Student's t test was utilized for comparing the quantitative and qualitative data. Inter- and intraobserver agreement were also assessed.

**RESULTS**
A total of 42 patients were included. The mean SSDE, $CTDI_{vol}$, contrast, noise, CNR, and SNR for SECT versus DECT were 12.7±2.2 mGy vs. 9.3±1.2 mGy ($P = 0.001$), 10.9±2.4 mGy vs. 8±1.2 mGy ($P < 0.001$), 211.9±44.7 vs. 216.3±59 ($P = 0.350$), 12.9±2.4 vs. 13.9±3.7 ($P = 0.086$), 13.5±5.2 vs. 13.3±8.4 ($P = 0.548$) and 12±3.5 vs. 11.5±3.4 ($P = 0.774$), respectively. Interobserver reproducibility was high for contrast, noise, CNR, and SNR (ICC = 0.89, 0.85, 0.93, and 0.82, respectively; all $P < 0.05$). Intraobserver reproducibility was high for contrast, noise, CNR, and SNR (ICC = 0.80, 0.77, 0.85, and 0.88, respectively; all $P < 0.05$).

**CONCLUSION**
The mean SSDE of the chest CTs obtained with FKS-DECT were 26.8% lower than those with SECT with significant difference for the objective assessment and there was no significant difference for the subjective assessment of the image qualities, in this series.

Dual-energy computed tomography (DECT) is a relatively newer development for routine clinical work with an increasing variety of applications (1, 2). Material decomposition, decreased beam hardening and scatter artifacts, and improved soft tissue contrast are the main advantages (3–6).

Single-energy CT (SECT) and DECT acquisitions are actually two completely different examination protocols that may be performed for different clinical indications. In DECT examination protocol, additional diagnostic information may be derived, which is not available in SECT. When clinically indicated, a DECT examination protocol should be employed. Apparently, the DECT examination protocol should be optimized in terms of radiation dose and image quality.

Different vendors provide different DECT techniques utilizing various technologies. These DECT techniques include dual rotation, dual source, fast kilovoltage-switching (FKS), and dual layered scanner systems (7). In FKS-DECT, the tube potential is continuously alternating from 80 kVp to 140 kVp every 0.25 ms, during the same tube rotation. (8). However, inability to utilize the automatic exposure control (AEC) is the major disadvantage and therefore, previous papers reported that FKS-DECT might be associated with higher radiation doses than the SECT (7–10). Thus, in the current study, we set out to compare the size-specific

From the Department of Radiology (O.M.T. ✉ *omtopcuoglu@gmail.com*) Yeditepe University School of Medicine, İstanbul, Turkey.

Received 11 September 2018; revision requested 7 October 2018; last revision received 3 November 2018; accepted 13 November 2018.

DOI 10.5152/dir.2019.18412

You may cite this article as: Topçuoğlu OM, Sarıkaya B. Fast kilovoltage-switching dual-energy CT offering lower x-ray dose than single-energy CT for the chest: a quantitative and qualitative comparison study of the two methods of acquisition. Diagn Interv Radiol 2019; 25:204–209.

dose estimates (SSDE), CT dose indices (CTDI$_{vol}$, in mGy) and image quality parameters of the chest CTs obtained with FKS-DECT versus those with SECT.

## Methods

### Patient population

Between October 2016 and October 2017, patients with lung malignancies who had contrast-enhanced chest CT with SECT within the last 6 months, were prospectively scanned with contrast-enhanced chest FKS-DECT for the routine follow-up imaging. Patients having chest CT without contrast were excluded. Demographic data, body mass indices (BMI), underlying diseases, the time interval between the two chest CTs and the CTDIs of both acquisitions were all noted. Local ethical committee approved the current study and written informed consent was obtained from all patients.

The underlying diseases were lung cancer (n=14), colorectal cancer (n=9), breast cancer (n=4), hepatocellular carcinoma (n=3), testis cancer (n=2), lymphoma (n=2) and others (n=8).

### SECT technique

All CT scans were obtained using a 64×2-slice multi-detector CT (3$^{rd}$ generation Revolution CT GSI with VE SW version; GE Healthcare). Patients were placed in supine position on the CT table and scanned in cranio-caudal direction. Routine chest CT protocol in our institute entails venous phase imaging of the chest, 65 s after the administration of 80–120 mL non-iodinated contrast material with a flow-rate of 3–4 mL/s from the antecubital vein, followed by 30 mL saline injection. Bolus-tracking technique was utilized for all CT scans. The following CT parameters were same for all SE scans: 64×0.625 mm collimation; 0.4 ms rotation time;1.375 pitch; 120 kVp tube potential; AEC tube current; 512×512 matrix; 1.25 mm slice thickness; 50% adaptive statistical iterative reconstruction (ASIR) (Table 1).

**Main points**

- The mean size-specific dose estimates and CT dose indices of the chest CTs obtained with fast kilovoltage-switching dual-energy CT (FKS-DECT) were lower than those with single-energy CT (SECT).
- FKS-DECT offers much lower x-ray dose than the SECT of the chest in obese patients with BMI greater than 30 kg/m$^2$.
- FKS-DECT of the chest had no significant difference compared with SECT in terms of image quality.

### DECT technique

All CT scans were obtained using a 64×2-slice multidetector CT (3$^{rd}$ generation Revolution CT GSI with VE SW version; GE Healthcare), the same CT scanner with the SECT. Patient positioning, contrast material administration and scan direction were exactly the same with the SECT scans. The following CT parameters were same for all DE scans: 64×0.625 mm collimation; 0.4 ms rotation time; 1.375 pitch; 80–140 kVp tube potential; 260–630 mA tube current; 512×512 matrix; 1.25 mm slice thickness; 50% ASIR (Table 1).

CTDI$_{vol}$ was obtained from patients' dose report given by the CT scanner at the end of the each acquisition.

### Quantitative assessment

All image assessments and measurements were made on local institutional radiology database. Dose length products (DLP) were not compared because the scan lengths were not identical for each protocol. Because the patient dose acquired from a CT examination is dependent on both patient size and CT radiation output, comparing only CTDI$_{vol}$ would be deficient and therefore, SSDE were also calculated. For SSDE calculations, water equivalent diameters derived from the sum of the patients' anterior-posterior and lateral dimensions, were multiplied with conversion factors based on the utilization of the 32 cm diameter acrylic (PMMA) phantom for CTDI$_{vol}$ (11). Absolute attenuation values in Hounsfield units (HU) were determined by drawing regions of interest (ROIs) of 120 mm$^2$ in the lumens of the ascending and descending aorta, main pulmonary artery, superior vena cava, right and left atrium, right and left ventricle, erector spina muscle, and subcutaneous fat tissue. The measurements were independently made twice by the two radiologists, each with more than 5 years of experience of interpreting chest CT images on the same screens and blinded to the technique used. Standard deviation (SD) values were also recorded. Contrast was defined as the difference of the mean HUs of the vascular bed and the cardiac spaces and the mean HU of the muscle; noise, as the mean SD of the subcutaneous fat tissue; contrast-to-noise ratio (CNR), as the ratio of the contrast to noise; and signal-to-noise ratio (SNR), as the ratio of the mean HUs of the vascular bed and the cardiac spaces to the mean SD of them (Table 2) (5, 12–16).

**Table 1.** Parameters for SECT and FKS-DECT protocols

| | CT acquisition | |
|---|---|---|
| CT parameter | SECT | FKS-DECT |
| Collimation (mm) | 64×0.625 | 64×0.625 |
| Rotation time (ms) | 0.4 | 0.4 |
| Pitch | 1.375 | 1.375 |
| Tube voltage (kVp) | 120 | 80–140 |
| Tube current (mA) | AEC (241–659) | 260–630* |
| Noise index | 30.28 | 29.20 |
| Kernel | Standard | Standard |
| Matrix | 512×512 | 512×512 |
| Slice thickness (mm) | 1.25 | 1.25 |
| Iterative reconstruction | 50% ASIR | 50% ASIR |
| Contrast volume (mL) | 80–120 | 80–120 |
| Injection rate (mL/s) | 3 | 3 |

CT, computed tomography; SECT, single-energy CT; FKS-DECT, fast kilovoltage-switching dual-energy CT; AEC, automatic exposure control; ASIR, adaptive statistical iterative reconstruction.
*Tube currents were 260 mA (n=6), 275 mA (n=13), 360 mA (n=21), 630 mA (n=2).

**Table 2.** Definitions of the contrast, noise, CNR, and SNR

| Parameter | Definition |
|---|---|
| Contrast | The difference of the mean HUs of the vascular bed and the cardiac spaces and the mean HU of the muscle |
| Noise | The mean SD of the subcutaneous fat tissue |
| CNR | Quotient of the contrast to the noise |
| SNR | The ratio of the mean HUs of the vascular bed and the cardiac spaces to the mean SD of them |

CNR, contrast-to-noise ratio; SNR, signal-to-noise ratio; HU, Hounsfield Unit; SD, standard deviation.

**Table 3.** The mean results of quantitative assessment

| Parameter | SECT | FKS-DECT | *P* |
|---|---|---|---|
| SSDE (mGy) | 12.7±2.2 | 9.3±1.2 | 0.001 |
| $CTDI_{vol}$ (mGy) | 10.9±.2.4 | 8±1.2 | <0.001 |
| Contrast | 211.9±44.7 | 216.3±59 | 0.350 |
| Noise | 12.9±2.4 | 13.9±3.7 | 0.086 |
| CNR | 13.5±5.2 | 13.3±8.4 | 0.548 |
| SNR | 12±3.5 | 11.5±3.4 | 0.774 |

SECT, single-energy CT; FKS-DECT, fast kilovoltage-switching dual-energy CT; SSDE, size-specific dose estimate; CTDI, CT dose index; CNR, contrast-to-noise ratio; SNR, signal-to-noise ratio.
Conversion factors calculating SSDE range between 1.01 and 1.40.

**Table 4.** The mean results of qualitative assessment (scored from 1 to 5)

| Parameter | SECT | FKS-DECT | *P* |
|---|---|---|---|
| Contrast | 3.9±1 | 4±0.8 | 0.678 |
| Noise | 3.4±0.7 | 3.6±0.6 | 0.902 |
| Vascular delineation | 3.7±1.1 | 3.6±0.9 | 0.337 |
| General image quality | 3.8±0.8 | 3.6±0.6 | 0.127 |

SECT, single-energy CT; FKS-DECT, fast kilovoltage-switching dual-energy CT.

### Qualitative assessment

Two radiologists, each with more than 5 years of experience in interpreting chest CT images, independently evaluated the SECT and DECT images of the chest on the same screens blinded to the technique used. Each interpreter scored the image contrast from 1 (lowest contrast) to 5 (highest contrast), noise from 1 (highest noise) to 5 (lowest noise), delineation of vessels within the mediastinum from 1 (almost cannot be differentiated) to 5 (clearly delineated), and the overall image quality from 1 (worst image quality) to 5 (best image quality) (14). The best image quality was defined as high contrast resolution, minimal or no noise, perfect attenuation of the vessel lumen and clear delineation of the vessel walls. Window width and window level were determined by the interpreters.

### Statistical analysis

To compare the SSDE, $CTDI_{vol}$, quantitative and qualitative data, the paired Student's t test was utilized. Descriptive statistics were expressed as mean±SD. The correlation between BMI and $CTDI_{vol}$ was assessed with Pearson correlation. Intraclass correlation coefficients were calculated for the intra- and interobserver agreement and values ≥0.75, 0.60–0.74, 0.40–0.59, and ≤0.40 were featured as high, good, fair, and poor agreement, respectively. $P < 0.05$ was considered as statistically significant. Statistical analysis was performed using IBM SPSS version 21 (IBM Corp.).

## Results

A total of 42 patients (26 men, 16 women) with a mean age of 59.5±11.7 years (range, 31–78 years) were enrolled in this prospective study. The mean BMI was 26.7±5.7 kg/m$^2$ (range, 16–46.3 kg/m$^2$). There were 19 patients with BMI ≤25 kg/m$^2$, 14 patients with BMI >25 and <30 kg/m$^2$, and 9 patients with BMI ≥30 kg/m$^2$. The mean time interval between the SECT and DECT of the chest was 6.2±4.4 months (range, 2–18 months).

The results of quantitative analysis were tabulated in Table 3. The conversion factors while calculating SSDE ranged between 1.01 and 1.40. Except SSDE and $CTDI_{vol}$, there were no significant differences between the two acquisitions in terms of quantitative measurements (Table 3). The radiation dose results obtained from both protocols were within the limits of diagnostic reference levels recommended by the American College of Radiology (17).

The mean SSDE, $CTDI_{vol}$, CNR, and SNR were compared between SECT and DECT of the chest: for patients with BMI ≤25 kg/m$^2$, SSDE was 11.8±1.4 mGy vs. 9.1±0.8 mGy ($P < 0.001$), $CTDI_{vol}$ was 9.9±1.4 mGy vs. 7.6±0.9 mGy ($P < 0.001$), CNR was 13.6±5.2 vs. 11±6.3 ($P=0.933$), and SNR was 12.3±4 vs. 10.6±3.5 ($P = 0.774$), respectively. For patients with BMI >25 to <30 kg/m$^2$, SSDE was 12.8±.1.9 mGy vs. 9.1±1.2 mGy ($P < 0.001$), $CTDI_{vol}$ was 10.8±.1.6 mGy vs. 7.7±0.9 mGy ($P<0.001$), CNR was 13.3±5.3 vs. 16.2±9.9 ($P = 0.166$) and SNR was 11.5±2.9 vs. 12.8±3 ($P=0.080$), respectively. For patients with BMI ≥30 kg/m$^2$, SSDE was 14.3±3.2 mGy vs. 10.1±1.4 mGy ($P=0.019$), $CTDI_{vol}$ was 13.3±3.7 mGy vs. 9.3±1.6 mGy ($P = 0.014$), CNR was 10.6±4.5 vs. 16.7±13.5 ($P = 0.138$), SNR was and 10.8±3.3 vs. 11.7±2.9 ($P = 0.240$), respectively.

Interobserver reproducibility was high for contrast, noise, CNR, and SNR (ICC=0.89, 0.85, 0.93 and 0.82, respectively; all $P < 0.05$). Intraobserver reproducibility was high for contrast, noise, CNR, and SNR (ICC=0.80, 0.77, 0.85 and 0.88, respectively; all $P < 0.05$).

The mean contrast, noise, vascular delineation, and overall image quality for SECT versus DECT were given in Table 4. There were no significant differences between the two acquisitions in terms of qualitative analysis (Table 4). Interobserv-

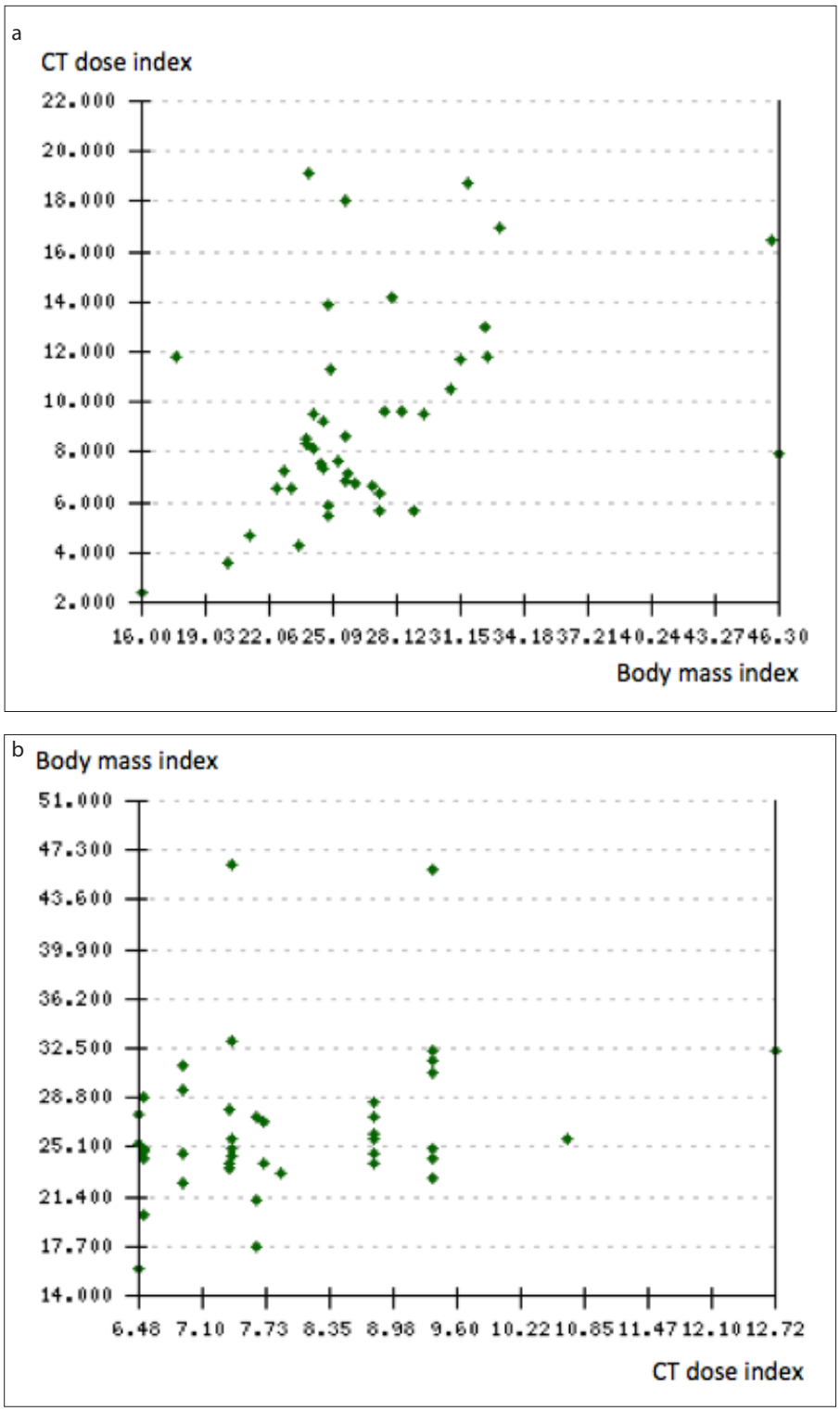


**Figure 1. a, b.** The relation between the CT dose index and the body mass index for the fast kilovoltage-switching dual-energy CT (FKS-DECT) **(a)** and single-energy CT (SECT) **(b)**.

er agreement was high for contrast and overall quality (ICC=0.77 and ICC=0.81, respectively, $P < 0.05$) and good for noise and vascular delineation (ICC=0.72 and ICC=0.67, respectively, $P < 0.05$). Intraobserver agreement was high for contrast, noise and overall quality (ICC=0.87, ICC=0.79, and ICC=0.93, respectively, $P < 0.05$) and good for vascular delineation (ICC=0.72, $P < 0.05$).

## Discussion

In FKS-DECT, the tube alternates rapidly between the two tube potentials (80–140 kVp) during the same rotation time, but the tube current cannot be changed simultaneously, which results in inability to use AEC (10). Therefore, it is assumed that the radiation dose of this DECT technique might be associated with higher radiation doses compared with SECT (7–10). However, the tube can alter the exposure time simultaneously to overcome this disadvantage and to achieve the maximum CNR (18, 19). Roughly 65% of the exposure time is utilized for the 80 kVp tube potential and 35% for the 140 kVp tube potential (18). The different exposure time ratios for the high and low tube voltages may compensate for the potential radiation dose increase, resulting from the lack of AEC. In the current study, we demonstrated that the SSDE and $CTDI_{vol}$ were 26.8% and 26.6% lower for FKS-DECT than SECT in the chest, respectively.

Although the FKS-DECT technique does not allow to use AEC, the current study also showed that using FKS-DECT for patients with BMI ≥30 kg/m$^2$ would be advantageous in terms of radiation dose compared to SECT. For patients with BMI ≥30 kg/m$^2$ in this series, SSDE and CTDIs were 29.4% and 29.1% lower for FKS-DECT than those for SECT, respectively, and the difference was statistically significant for SSDE. The relation between the $CTDI_{vol}$ and the BMI for the FKS-DECT and the SECT was shown in Fig. 1.

Today, practically all CT systems utilize the AEC enabling the tube current modulation in three dimensions (20). Basically, it increases or decreases the tube current, thus increasing and decreasing the dose according to the thickness of the body parts and the organs scanned. Many previous papers including both phantom and patient studies showed that with the utilization of AEC, there was a significant radiation exposure reduction to the patient up to 60% (20–24). However, in the current study, the mean SSDE and $CTDI_{vol}$ of SECT of the chest using AEC were found to be 23.9%, 26.8%, 29.4% and 23.3%, 26.6%, 29.1% more than those of FKS-DECT for the patients with BMI ≤25 kg/m$^2$, >25 and <30 kg/m$^2$, and ≥30 kg/m$^2$, respectively. Significant difference was detected between the two acquisitions regarding SSDE and $CTDI_{vol}$, and there was no significant difference in terms of other quantitative (except SSDE and $CTDI_{vol}$) and qualitative image quality parameters. The

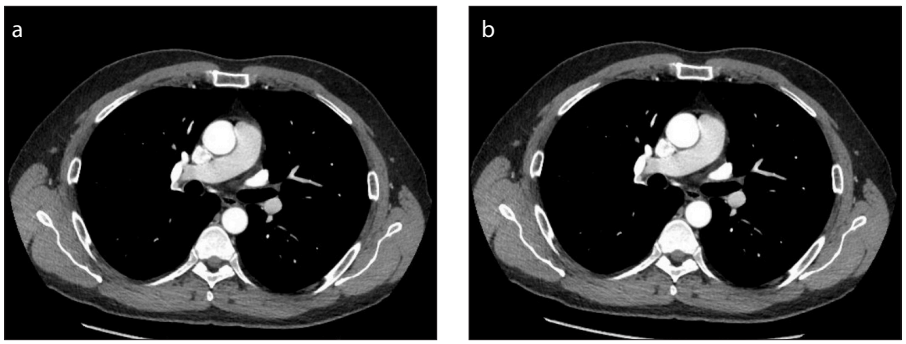


**Figure 2. a, b.** Axial CT images from FKS-DECT **(a)** versus SECT of the chest **(b)**.

main reason for the increment of SSDE and $CTDI_{vol}$ along with the BMI for the SECT, might be due to the use of AEC, because the tube current was automatically increased with the increased patient thickness. Thus, as the patient thickness increased, the BMI and the tube current and so the radiation dose increased. However, in FKS-DECT the tube current was constant and it could be set by the user as low as 260 mA to remain the same for the whole scan length. Geyer et al. (25) found significantly higher doses for FKS-DECT of the chest over dual source DECT. However, they selected the tube current as high as 630 mA and therefore, higher radiation doses became inevitable. Although they have opted to use higher tube current values, our study demonstrated that it could be set as low as possible without loss of image quality.

Although FKS-DECT technique utilizes alternating two different energies including one higher energy (140 kVp), the radiation dose does not become doubled. Our prospective study demonstrated that when other CT parameters are kept constant, even though there was no statistically significant difference between the two acquisitions in terms of image quality parameters, the $CTDI_{vol}$ for the FKS-DECT of the chest was 26.6% lower than those for SECT. Li et al. (18) found the $CTDI_{vol}$ 22% more for FKS-DECT than SECT. However, their study was a phantom study and it aimed to compare the $CTDI_{vol}$ of FKS-DECT and SECT for head and body examinations. The current study is the first report comparing SSDE and $CTDI_{vol}$ of FKS-DECT and SECT of the chest. Ho et al. (26) reported two to three times higher radiation doses for FKS-DECT. However, their DECT set-up lacked optimization of the exposure time ratios for the alternating energies and the gantry revolution times were not identical for SECT and DECT protocols and it was nearly two times slower for FKS-DECT. In contrast, the gantry revolution times were identical in our study. Therefore, longer gantry revolution times of first generation FKS-DECT result in significantly higher radiation doses and hamper its routine clinical utilization.

A robust assessment and comparison of two different acquisition systems should be based on a benchmark of the radiation dose required to achieve a similar image quality (27). In other words, the radiation dose should be as low as reasonably achievable (ALARA) while performing high quality images (28). Buty et al. (29) reported that diminished-dose DECT had no significant image quality difference compared with standard-dose CT by using a dual source DECT. The current study also showed that the image quality parameters were not significantly different both subjectively and objectively between FKS-DECT and SECT of the chest (Fig. 2). Li et al. (18) found the image noise 30% lower for FKS-DECT than SECT in a phantom study. Previous papers reported that the achieved image qualities were similar as in our study; but unlike our study, the radiation doses were found to be 22% and 14% higher for FKS-DECT than SECT in the head and body examinations (18, 30, 31). Zhang et al. (32) reported that spatial resolution, image noise, and CNR were equivalent for FKS-DECT and SECT in abdominal imaging.

There were several limitations in the current study. First of all, the total number of the patients remained low, thus it is not possible to draw robust conclusions. Second, the subjective assessment of the images were made without a consensus method but the interobserver agreements remained high or good. Third, although we used the same injection rate and the same contrast volume for the same patient, the hemodynamic status of the patient might potentially influence the CNR for DECT and SECT acquisitions. Finally, the main limitation was the user dependency of the tube current for FKS-DECT and we set the tube current as low as possible for the DECT protocol, with the preservation of the image quality, which might hamper reproducible results.

In conclusion, our findings showed that the mean SSDE of the chest CTs obtained with FKS-DECT was significantly (26.8%) lower than those with SECT, with no significant difference in the subjective assessment of the image qualities.

## Conflict of interest disclosure

The authors declared no conflicts of interest.

## References

1. Schoepf UJ and Colletti PM. New dimensions in imaging: the awakening of dual-energy CT. AJR Am J Roentgenol 2012; 199:S1–2. [CrossRef]
2. Flohr TG, McCollough CH, Bruder H, et al. First performance evaluation of a dual-source CT (DSCT) system. Eur J Radiol 2006; 16:256–268. [CrossRef]
3. Meier A, Wurnig M, Desbiolles L, et al. Advanced virtual monoenergetic images: improving the contrast of dual-energy CT pulmonary angiography. Clin Radiol 2015; 70:1244–1251. [CrossRef]
4. Bamberg F, Dierks A, Nikolaou K, et al. Metal artifact reduction by dual energy computed tomography using monoenergetic extrapolation. Eur J Radiol 2011; 21:1424–1429. [CrossRef]
5. Apfaltrer P, Sudarski S, Schneider D, et al. Value of monoenergetic low-kV dual energy CT datasets for improved image quality of CT pulmonary angiography. Eur J Radiol 2014; 83:322–328. [CrossRef]
6. Pessis E, Campagna R, Sverzut JM, et al. Virtual monochromatic spectral imaging with fast kilovoltage switching: reduction of metal artifacts at CT. Radiographics 2013; 33:573–583. [CrossRef]
7. Otrakji A, Digumarthy SR, Lo Gullo R, et al. Dual-energy CT: spectrum of thoracic abnormalities. Radiographics 2016; 36:38–52. [CrossRef]
8. Agrawal MD, Pinho DF, Kulkarni NM, et al. Oncologic applications of dual-energy CT in the abdomen. Radiographics 2014; 34:589–612. [CrossRef]
9. Silva AC, Morse BG, Hara AK, et al. Dual-energy (spectral) CT: applications in abdominal imaging. Radiographics 2011; 31:1031–1046. [CrossRef]
10. Kaza RK, Platt JF, Cohan RH, et al. Dual-energy CT with single- and dual-source scanners: current applications in evaluating the genitourinary tract. Radiographics 2012; 32:353–369. [CrossRef]
11. American Association of Physicists in Medicine. Use of water equivalent diameter for calculating patient size and size-specific dose estimates (SSDE) in CT: report of AAPM Task Group 220. College Park, Md: American Association of Physicists in Medicine, 2014.

12. Schneider D, Apfaltrer P, Sudarski S, et al. Optimization of kiloelectron volt settings in cerebral and cervical dual-energy CT angiography determined with virtual monoenergetic imaging. Acad Radiol 2014; 21:431–436. [CrossRef]
13. Albrecht MH, Scholtz JE, Husers K, et al. Advanced image-based virtual monoenergetic dual-energy CT angiography of the abdomen: optimization of kiloelectron volt settings to improve image contrast. Eur J Radiol 2016; 21:1863–1870. [CrossRef]
14. Doerner J, Hauger M, Hickethier T, et al. Image quality evaluation of dual-layer spectral detector CT of the chest and comparison with conventional CT imaging. Eur J Radiol 2017; 93:52–58. [CrossRef]
15. Schenzle JC, Sommer WH, Neumaier K, et al. Dual energy CT of the chest: how about the dose? Invest Radiol 2010; 45:347–353. [CrossRef]
16. Zhu X, McCullough WP, Mecca P, et al. Dual-energy compared to single-energy CT in pediatric imaging: a phantom study for DECT clinical guidance. Pediatr Radiol 2016; 46:1671–1679. [CrossRef]
17. Kanal KM, Butler PF, Sengupta D, et al. U.S. diagnostic reference levels and achievable doses for 10 adult CT examinations. Radiology 2017; 284:120–133. [CrossRef]
18. Li B, Yadava G and Hsieh J. Quantification of head and body CTDI(VOL) of dual-energy x-ray CT with fast-kVp switching. Med Phys 2011; 38:2595–2601. [CrossRef]
19. Machida H, Fukui R, Tanaka I, et al. A method for selecting a protocol for routine body CT scan using Gemstone Spectral Imaging with or without adaptive statistical iterative reconstruction: phantom experiments. Jpn J Radiol 2014; 32:217–223. [CrossRef]
20. Soderberg M and Gunnarsson M. Automatic exposure control in computed tomography--an evaluation of systems from different manufacturers. Acta Radiol 2010; 51:625–634. [CrossRef]
21. Mulkens TH, Bellinck P, Baeyaert M, et al. Use of an automatic exposure control mechanism for dose optimization in multi-detector row CT examinations: clinical evaluation. Radiology 2005; 237:213–223. [CrossRef]
22. Verdun FR, Gutierrez D, Schnyder P, et al. CT dose optimization when changing to CT multi-detector row technology. Curr Probl Diagn Radiol 2007; 36:176–184. [CrossRef]
23. Rizzo S, Kalra M, Schmidt B, et al. Comparison of angular and combined automatic tube current modulation techniques with constant tube current CT of the abdomen and pelvis. AJR Am J Roentgenol 2006; 186:673–679. [CrossRef]
24. Papadakis AE, Perisinakis K and Damilakis J. Automatic exposure control in pediatric and adult multidetector CT examinations: a phantom study on dose reduction and image quality. Med Phys 2008; 35:4567–4576. [CrossRef]
25. Geyer LL, Scherr M, Korner M, et al. Imaging of acute pulmonary embolism using a dual energy CT system with rapid kVp switching: initial results. Eur J Radiol 2012; 81:3711–3718. [CrossRef]
26. Ho LM, Yoshizumi TT, Hurwitz LM, et al. Dual energy versus single energy MDCT: measurement of radiation dose using adult abdominal imaging protocols. Acad Radiol 2009; 16:1400–1407. [CrossRef]
27. Forghani R, De Man B and Gupta R. Dual-energy computed tomography: physical principles, approaches to scanning, usage, and implementation: Part 2 Neuroimaging. Clin N Am 2017; 27:385–400. [CrossRef]
28. Lam S, Gupta R, Kelly H, et al. Multiparametric evaluation of head and neck squamous cell carcinoma using a single-source dual-energy CT with fast kVp switching: state of the art. Cancers 2015; 7:2201–2216. [CrossRef]
29. Buty M, Xu Z, Wu A, et al. Quantitative image quality comparison of reduced- and standard-dose dual-energy multiphase chest, abdomen, and pelvis CT. Tomography 2017; 3:114–122. [CrossRef]
30. Kamiya K, Kunimatsu A, Mori H, et al. Preliminary report on virtual monochromatic spectral imaging with fast kVp switching dual energy head CT: comparable image quality to that of 120-kVp CT without increasing the radiation dose. Jpn J Radiol 2013; 31:293–298. [CrossRef]
31. Hwang WD, Mossa-Basha M, Andre JB, et al. Qualitative comparison of noncontrast head dual-energy computed tomography using rapid voltage switching technique and conventional computed tomography. J Comput Assist Tomogr 2016; 40:320–325. [CrossRef]
32. Zhang D, Li X and Liu B. Objective characterization of GE discovery CT750 HD scanner: gemstone spectral imaging mode. Med Phys 2011; 38:1178–1188. [CrossRef]